SLURRY F-T REACTOR HYDRODYNAMICS AND SCALE-UP

DEPARTMENT OF ENERGY, PITTSBURGH, PA.
PITTSBURGH ENERGY TECHNOLOGY CENTER

1984

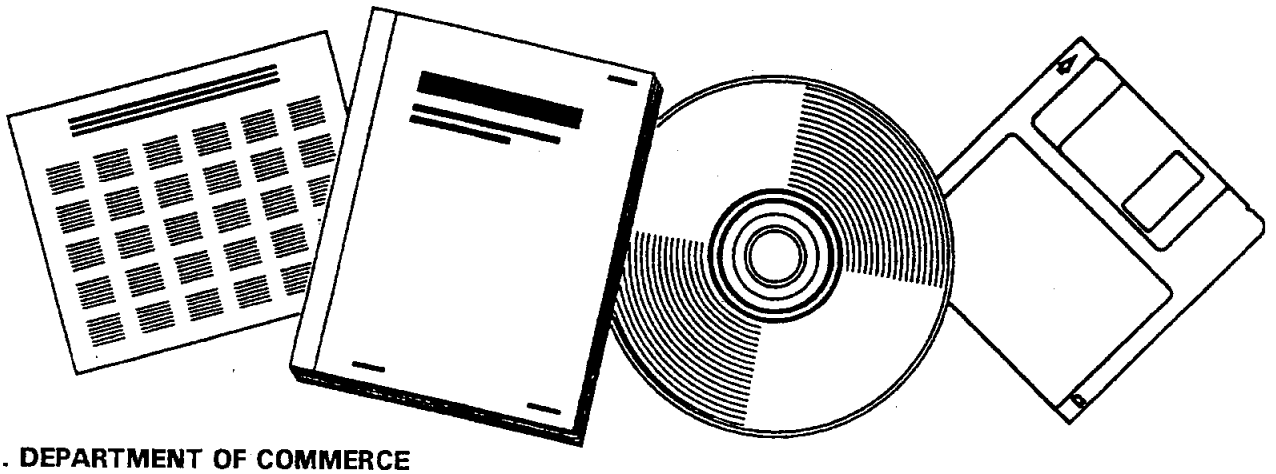

U.S. DEPARTMENT OF COMMERCE
National Technical Information Service

CONF-8410328--1

CONF-8410328--1

DE85 013227

Fourth DOE Contractors' Conference Indirect Liquefaction

October 30-31, 1984

Holiday Inn/Meadowlands
Washington, Pennsylvania

Slurry F-T Reactor Hydrodynamics and Scale-Up

by

Dennis N. Smith, William O'Dowd, John A. Ruether, and Gary J. Stiegel

Pittsburgh Energy Technology Center

P.O. Box 10940

Pittsburgh, Pennsylvania 15236

and

Yatish T. Shah

University of Pittsburgh

1249 Benedum Hall

Pittsburgh, Pennsylvania 15261

ABSTRACT

The Fischer-Tropsch (F-T) synthesis of hydrocarbons by the hydrogenation of carbon monoxide over a catalyst via the indirect liquefaction route has only been demonstrated on a commercial scale in fixed-bed and entrained-bed reactors. The slurry reactor has been found to offer important advantages, such as low H_2/CO feed ratios and isothermal stability on the laboratory and pilot-plant scale. Recent findings concerning slurry bubble column hydrodynamics are presented, and their relevance to slurry F-T reactor design and scale-up are discussed. The need for optimization of a slurry F-T reactor is apparent owing in large part to the nonselective formation of products on the catalyst, and the influence of hydrodynamics on the overall conversion of reactants. In this regard, the important transport resistances in the formation of products, and the influence of reactor dimensions on reactor performance are discussed.

INTRODUCTION

Design of a slurry bubble column reactor requires reliable estimation of transport parameters influencing the overall reactor performance. The Fischer-Tropsch synthesis is thought to occur in the slow-reaction regime, which is advantageous for slurry reactor applications because of low power consumption per unit volume and isothermal stability. The critical parameters for the design and scale-up of F-T slurry reactors are the following: gas holdup, distribution of solid catalyst, intrinsic kinetics, flow regime transition, fluid mixing, gas-liquid interfacial area, and volumetric mass transfer coefficient. The present communication addresses some hydrodynamic parameters that are poorly understood and the difficulty in extrapolation of these parameters obtained from "cold-model" data to a commercial F-T slurry reactor.

Recent studies by Mobil (Kuo et al., 1983) indicate that under F-T reaction conditions, gas holdups are obtained that are significantly higher than those predicted from the literature. The large gas holdup is thought to be due to surface-active impurities in the liquid phase that may or may not cause foaming to occur. The bubble dynamics and its effect on the hydrodynamics of liquid mixtures containing surface-active impurities are not presently well understood. The following discussion presents data obtained from a 10-cm-diameter cold model that compares gas holdup, flow regime transitions, axial solids concentration distributions, and bubble size distributions for foaming and nonfoaming liquid systems. Important differences between these two types of liquid systems are identified, and

the implications of these differences on F-T slurry hydrodynamics and scale-up are addressed.

EXPERIMENTAL

A 10-cm-diameter bubble column equipped with two types of distributors (perforated plate with 1-mm x 76 holes and sintered plate with 20-μm nominal hole size) has been used to obtain gas holdup, bubble size distributions, and axial solids concentration distributions. The liquids used in this study were water, mixtures of water/ethanol, and a low-viscosity silicone oil (μ_L = 0.8 cp). The solids used were narrow-sized glass beads having a mean particle size of 96.5 μm.

Gas holdup was obtained from the level difference of aerated and stagnant liquid. Bubble size distributions were measured in situ with a miniaturized conductivity probe (Smith et al., 1984). Axial solids concentration distributions were obtained from slurry samples taken at six axial positions in 35-cm intervals beginning at 5 cm from the distributor plate. Details of the experimental procedure and method of analysis are given elsewhere (Smith and Ruether, 1984; Shah et al., 1984).

RESULTS

Gas Holdup

The aim of investigating gas holdup in the present study was to consider the effect of foaming and nonfoaming liquid systems, and the resulting

change in local and average gas holdup. Local gas holdup was measured as a function of axial and radial position with a miniaturized conductivity probe (Smith et al., 1984).

Figure 1 shows the effect of the distributor type on gas holdup for nonfoaming liquids having a low surface tension (18.7 dyne/cm). For the low surface tension liquid (silicone oil), gas holdup is similar for both types of distributor. This implies that for nonfoaming liquids having a low surface tension, the effect of distributor type is very small.

In Figure 2, the effect of distributor type on gas holdup for foaming liquids is shown to be very significant. For gas velocities between 1 and 10 cm/s, the gas holdup with the sintered plate was substantially higher than for the perforated-plate distributor. In the range of gas velocities used by Mobil's F-T reactor (Kuo et al., 1983), the gas holdup obtained with the ethanol/water mixture is almost the same as that obtained in the F-T reactor. Since both columns were equipped with similar distributor plates, it is reasonable to expect that F-T liquids have behavior similar to that of the ethanol/water mixture shown in Figure 2 over a comparable range of gas velocities.

Figure 3 demonstrates the effect of ethanol/water composition on gas holdup for a range of gas velocities reported by Shah et al., 1984. These data were obtained in a 10-cm-diameter bubble column equipped with a 20-μm nominal diameter distributor plate. The gas holdup increases significantly when the ethanol concentration is between 0.47 wt% and 41 wt% and the gas velocity is greater than 2.5 cm/s. Below or above these concentrations, the

gas holdup is relatively insensitive to changes in ethanol concentration. This behavior is qualitatively predicted by the dynamic surface tension model of Andrew (1960).

Figures 4 and 5 show the radial distribution of gas holdup for water and 48-wt% aqueous ethanol systems, respectively. The local gas holdups were measured with an electrical conductivity probe at a superficial gas velocities of 3.1 cm/s and 9.0 cm/s. The radial profiles indicate that a parabolic distribution approximately describes the gas holdups, with a maximum gas holdup located near the center of the column and a gas holdup approaching 0 at the wall. The effect of gas velocity on the radial gas holdup profile is shown in Figure 4. With an increase in gas velocity, the volume of the gas phase occupying the central region of the bubble column increases, along with a corresponding sharp decrease in holdup near the wall. In Figure 5, the radial gas holdup profile for 48-wt% aqueous ethanol is shown at a gas velocity of 3.1 cm/s. The radial profile is observed to be flatter than for similar conditions obtained with the water system. This is most likely a result of a reduced coalescence rate of the bubbles in the ethanol/water mixture, which reduces the variance in the bubble size distribution and consequently provides a more uniform radial distribution of gas holdup.

Bubble Lengths

Bubble lengths were determined from measurements made with a twin conductivity probe and data acquisition/analysis system. The bubble length distributions were interpreted according to the probability model suggested

by Tsutsui and Miyauchi (1980). A log-normal distribution of bubble size is assumed and the probability factors used to interpret the relationship between bubble length and bubble size are given by Hess (1983). The calculated cumulative frequency distributions of bubble lengths are compared to the experimental values in Figures 6 through 8.

Figures 6 and 7 contrast the effect of gas velocity on the bubble length distribution for a coalescing system. As the gas velocity is increased from 3.1 cm/s to 9.0 cm/s, the frequency of the measured bubble lengths smaller than 1 mm more than doubles. In addition, the frequency of bubble lengths larger than 7 mm also increases with an increase in gas velocity. This dual increase in the frequency of large and small bubbles may partially explain why these results and those in the literature indicate that the Sauter mean bubble diameter does not increase with increasing gas velocity. It has been shown elsewhere (Smith et al., 1984) that the Sauter mean bubble size is 1.5 times the average bubble length for a log-normal distribution of bubble sizes.

In Figure 8, the cumulative frequency distribution for the 48-wt% aqueous ethanol system is shown. The results show that nearly all of the lengths measured were less than 7 mm. The percentage of bubble lengths smaller than 2 mm is greater than 65, and the percentage of bubble lengths smaller than 1 mm is approximately 50. A comparison of Figures 6 and 8 show that, at a superficial gas velocity of 3.1 cm/s, the percentage of bubble lengths less than 1 mm for the aqueous ethanol system is approximately 2.5 times greater than for the water system. This marked change in bubble size

is related to the noncoalescing nature of the bubbles in a surface-active liquid mixture.

The assumption of a log-normal distribution of bubble sizes accurately describes the noncoalescing aqueous ethanol system and the water system at low gas velocities. However, when the gas velocity in the water system surpasses 9 cm/s the log-normal distribution no longer gives an accurate description. This result may be related to inaccuracies of measuring bubble lengths at the higher flow rates (i.e., all the bubbles may not be observed) or it may indicate that a different distribution of bubble sizes exists (i.e., bimodal distribution).

Bubble Flow Regime

The bubble flow regime for F-T reactors must be adequately characterized because of the relatively low gas velocities normally employed (less than 10 cm/s). In the homogeneous bubble flow regime, the bubbles travel at nearly constant velocity with a small degree of mixing. Under these conditions, the gas holdup is adequately described with one parameter, the terminal bubble rise velocity. A force balance for the bubbles in the homogeneous bubble flow regime was performed by Marrucci (1965), and the following expression for terminal bubble rise velocity can be derived from his work:

$$U_{b\infty} = \frac{\bar{U}_g \ (1-\varepsilon_g^{5/3})}{\varepsilon_g \ (1-\varepsilon_g)} \qquad (1)$$

Equation (1) can be used when the bubble Reynolds number is less than 300. By taking the limit as $\epsilon_g \rightarrow 1$ in Equation (1), the following equation for maximum gas velocity in the bubble flow regime can be derived:

$$\bar{U}_g(max) = 0.6\ U_{b\infty} \qquad (2)$$

In practical applications, the transition from the bubble flow regime occurs at much lower gas velocities than those prediced by Equation (2), especially for liquid systems that do not inhibit bubble coalescence.

Figures 9 and 10 show how the terminal bubble rise velocity is calculated for a nonfoaming and a foaming system, respectively. In both systems, Equation (1) holds up to gas velocities of approximately 3 cm/s. The slope represents the reciprocal of the terminal bubble rise velocity. Above gas velocities of 3 cm/s, the two systems behave differently. The nonfoaming system (water) shows a sudden decrease in slope with increasing gas velocity, indicating a sudden increase in the bubble rise velocity (Figure 9). The foaming system (1.8-wt% aqueous ethanol) exhibits just the opposite behavior (Figure 10). The bubble rise velocity initially decreases with an increase in gas velocity above 3 cm/s and then increases near the theoretical limit of gas velocity for the bubble flow regime.

The terminal bubble rise velocities for a wide range of concentrations of ethanol in water are shown in Table 1. With small concentrations of ethanol in water, the terminal velocity decreases slightly. Further

increases in ethanol concentration have little effect on the terminal bubble rise velocity.

An example of the prediction of gas holdup in the bubble flow regime using Equation (1) is shown in Figure 11. For gas velocities less than 2.5 cm/s, the values of gas holdup obtained from Equation (1) show good agreement with the experimental values. However, as the gas velocity is increased beyond 2.5 cm/s, Equation (1) greatly underpredicts the gas holdup. This sudden increase in holdup is a result of the foaming capacity of the aqueous butanol system used in this case. With the sudden increase in gas holdup, several phenomena occur. A marked increase in gas and liquid circulation is observed, and the flow structure of the gas phase varies with axial position. At the top of the column, the gas bubbles are large and divided by thin liquid films. Throughout the rest of the column, the gas phase consists of very small bubbles. These small bubbles are well mixed and display higher velocities at the centerline of the column diameter and predominantly downward flow near the walls. A theoretical description of the flow regime transition for foaming and nonfoaming liquids has been given by Shah et al. (1984). A prediction of the onset of foaming is given by the following expression:

$$Fr_g = 0.25\ \varepsilon_g^{\,2}/(1-\varepsilon_g^{\,3/2}) \qquad (3)$$

This simple criteria for the prediction of the onset of foaming has been tested successfully with data obtained from the aqueous ethanol systems

and also with the data obtained with FT-200 wax in a F-T reactor hot model (Kuo et al., 1983).

Axial Solids Concentration Distributions

The axial solids or catalyst concentration distribution in F-T slurry reactors is expected to be relatively uniform for commercial-scale equipment. However, pilot-plant reactors are known to have significant variations in solids concentration along the length of the column that are greater than would be expected from predictions available in the literature. This implies that the hindered-settling velocity and/or the solids mixing rate are different for F-T slurry reactors and reactor to cold models. For this reason, axial solids concentration distributions were measured with foaming and nonfoaming liquids to determine if surface-active components in the liquid could alter the mixing and settling rates of the solids.

Figures 12 and 13 contrast the axial solids concentration distributions for water and 1.8-wt% aqueous ethanol systems. Figure 12 shows that at a low gas velocity, 3.1 cm/s, the axial solids concentration distribution is only slightly affected by the liquid foaming tendency. However, in Figure 13, at a superficial gas velocity of 15.0 cm/s, the axial solids concentration distribution has a much larger variance for the 1.8-wt% ethanol/water mixture (foaming system) as compared to the water system. Even though the bulk liquid properties are nearly the same for the two liquid systems, the flow behaviors of the foaming and nonfoaming systems are markedly different.

This increase in variance of solids distribution for the foaming liquid is in qualitative agreement with the variance of catalyst distribution for F-T slurry reactors. This further supports the hypothesis that F-T liquids may have foaming capacity.

The measured axial solids concentration distributions were analyzed with a sedimentation-dispersion model (Smith et al., 1984) to determine the hindered-settling velocity (U_p) and solids dispersion coefficient (E_s). The differential mass balance of the solids may be expressed as follows:

$$\frac{-E_s}{L}\frac{dC_s}{dx} + (U_{sL} - \bar{\Psi}_L U_p)C_s = U_{sL}C_s^{\epsilon} \qquad (4)$$

Equation (4) may be integrated to provide an analytical expression for axial solids concentration as a function of measurable operating variables and two hydrodynamic parameters (U_p and E_s). Figure 14 shows the result of this analysis for the solids dispersion coefficient. The Figure illustrates the effects of gas velocity and liquid type on the solids dispersion coefficient. The solids dispersion coefficient increases with an increase in gas velocity for both liquid systems. However, the solids dispersion coefficient for the foaming system (1.8-wt% aqueous ethanol) is significantly lower than for the nonfoaming liquid (water), especially at higher gas velocities. This implies that mixing in a foaming liquid may be lower than for a nonfoaming liquid and could offer distinct advantages for achieving higher conversions in an F-T slurry reactor as the diameter of the reactor is increased. The extent of fluid and catalyst mixing is poorly

understood at present and needs to be further investigated, especially in columns of larger diameters.

DISCUSSION

At present, the state-of-the-art design of F-T slurry reactors can be most dramatically improved with improvements in catalyst performance. Areas of catalyst development include improvements in catalyst selectivity, activity maintenance, and increased intrinsic reaction rates. To take advantage of potential improvements in catalyst performance, the knowledge of hydrodynamic parameters must be improved for F-T slurry systems at reaction conditions. Clearly F-T liquids appear to have a foaming capacity that alters the hydrodynamic performance of the reactors, which cannot be readily evaluated from transport parameters available in the literature. A pressing issue not yet resolved is the extent of foaming that F-T slurries exhibit at higher gas velocities. Almost catagorically, the studies of gas-phase behavior in F-T liquids have been performed at low gas velocities (less than 5 cm/s). In our studies with foaming liquids, we find that the greatest changes in hydrodynamic parameters occur at gas velocities greater than 3 cm/s. Further studies are urgently needed at higher gas velocities (up to 15 cm/s) in F-T liquids at reaction conditions, since higher velocities are expected to be used in scaled-up F-T slurry reactors.

NOMENCLATURE

C_s = solids concentration in slurry, kg/m^3

C_s^f = solids concentration in slurry feed kg/m^3

D = column diameter, m

E_s = axial solids dispersion coefficient, m^2/s

Fr_g = Froude number of gas phase ($\bar{U}_g/\sqrt{gD}$)

g = gravitational acceleration, m/s^2

L = length of column, m

$U_{b\infty}$ = terminal bubble rise velocity, m/s

$\bar{U}_g$ = superficial gas velocity, m/s

U_p = hindered-settling velocity, m/s

U_{sL} = slurry velocity, m/s

X = dimensionless axial position

z = axial position from bottom of column, m

Greek Symbols

ϵ_g = gas holdup

$\bar{\epsilon}$ = average liquid fraction in slurry

REFERENCES

1. Kuo, J.C.W., "Slurry Fischer-Tropsch/Mobil Two-Stage Process of Converting Syngas to High Octane Gasoline," Final Report DOE/PC/30022-10, June 1983.

2. Smith, D.N., Fuchs, W., Lynn, R.J., Smith, D.H., and Hess, M., "Bubble Behavior in a Slurry Bubble Column Reactor," ACS Symp. Ser. 237, Chemical and Catalytic Reactor Modeling, M.P. Dudukvic and P.L. Millo, eds., 125-147, 1984.

3. Smith, D.N., and Ruether, J.A., "Dispersed Solids Dynamics in a Slurry Bubble Column," accepted by Chem. Eng. Sci., 1984.

4. Shah, Y.T., Joseph, S., Smith, D.N., and Ruether, J.A., "On the Behavior of the Gas Phase in a Bubble Column with Ethanol-Water Mixtures," submitted to Ind. Eng. Chem., Process Des. Develop., 1984.

5. Andrew, S.P.S., "Frothing in Two-Component Liquid Mixtures," International Symposium on Distillation, Instr. Chem. Engrs., 73-78, 1960.

6. Tsutsui, T., and Miyauchi, T., "Fluidity of a Fluidized Catalyst Bed and Its Effect on the Behavior of the Bubbles," Int. Chem. Eng. 20, 386-393, 1980.

7. Hess, M., "Alternate Distribution Functions of Bubble Diameters Log-Normal and Log-Gamma Distribution Functions," Final Report DE-AP22-83PC10614, July 1983.

8. Marrucci, G., "Rising Velocity of a Swarm of Spherical Bubbles," Ind. Eng. Chem., Fundam. 4, 224-5, 1965.

9. Smith, D.N., Ruether, J.A., Stiegel, G.J., and Shah, Y.T., "A Modified Sedimentation-Dispersion Model for Solids Behavior in Coal Liquefaction Reactor," to be presented at the Annual AIChE Meeting, San Francisco, Calif. (November 25-30, 1984).

TABLE 1.

TERMINAL BUBBLE VELOCITY FOR H_2O-ETOH SYSTEM

Wt. % Ethanol	$U_{b\infty}$, CM/S
0	20.7
0.047	18.2
1.84	17.6
15.6	17.6
93.7	19.2

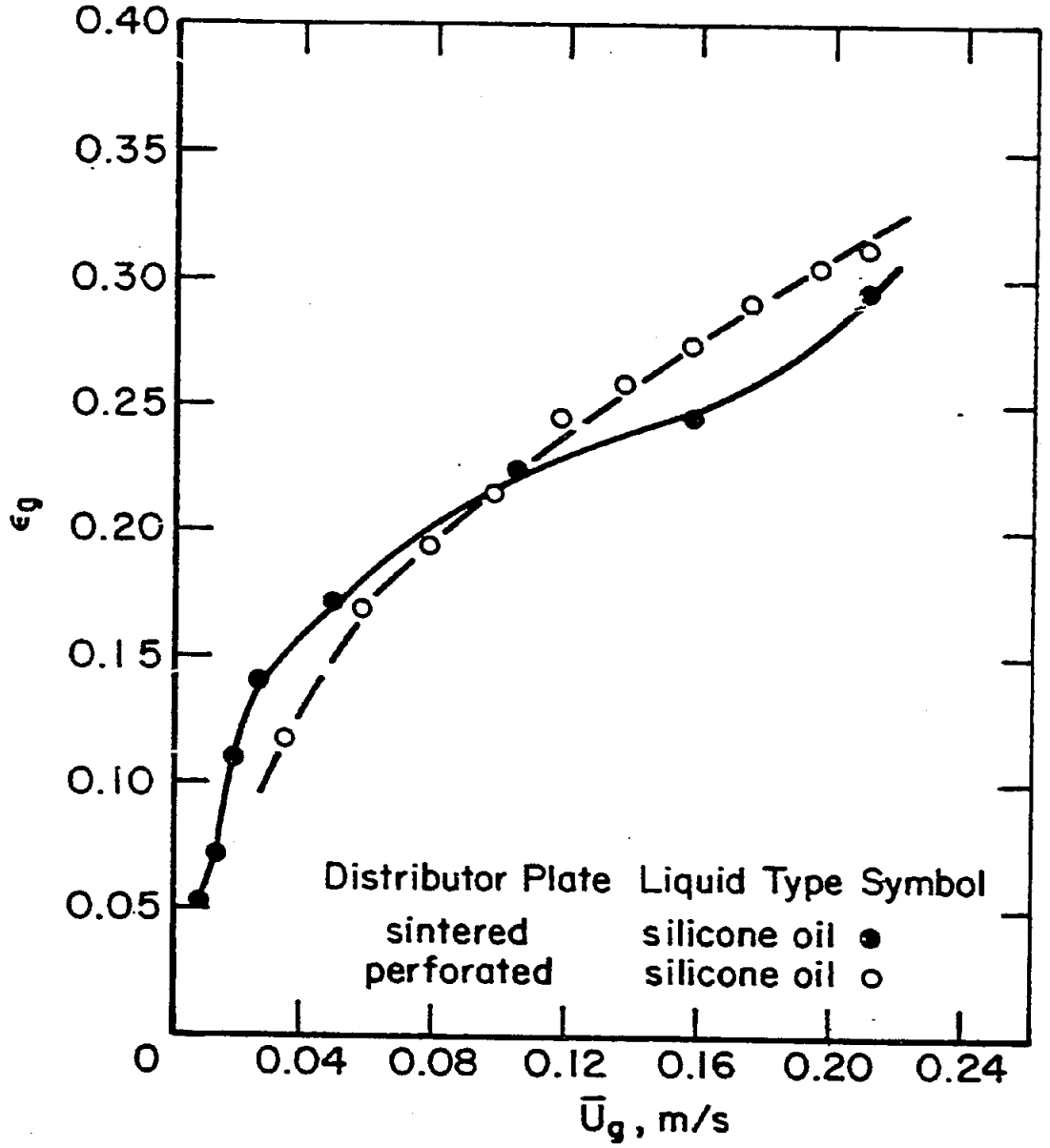

Figure 1. Effect of distributor type for nonfoaming liquids.

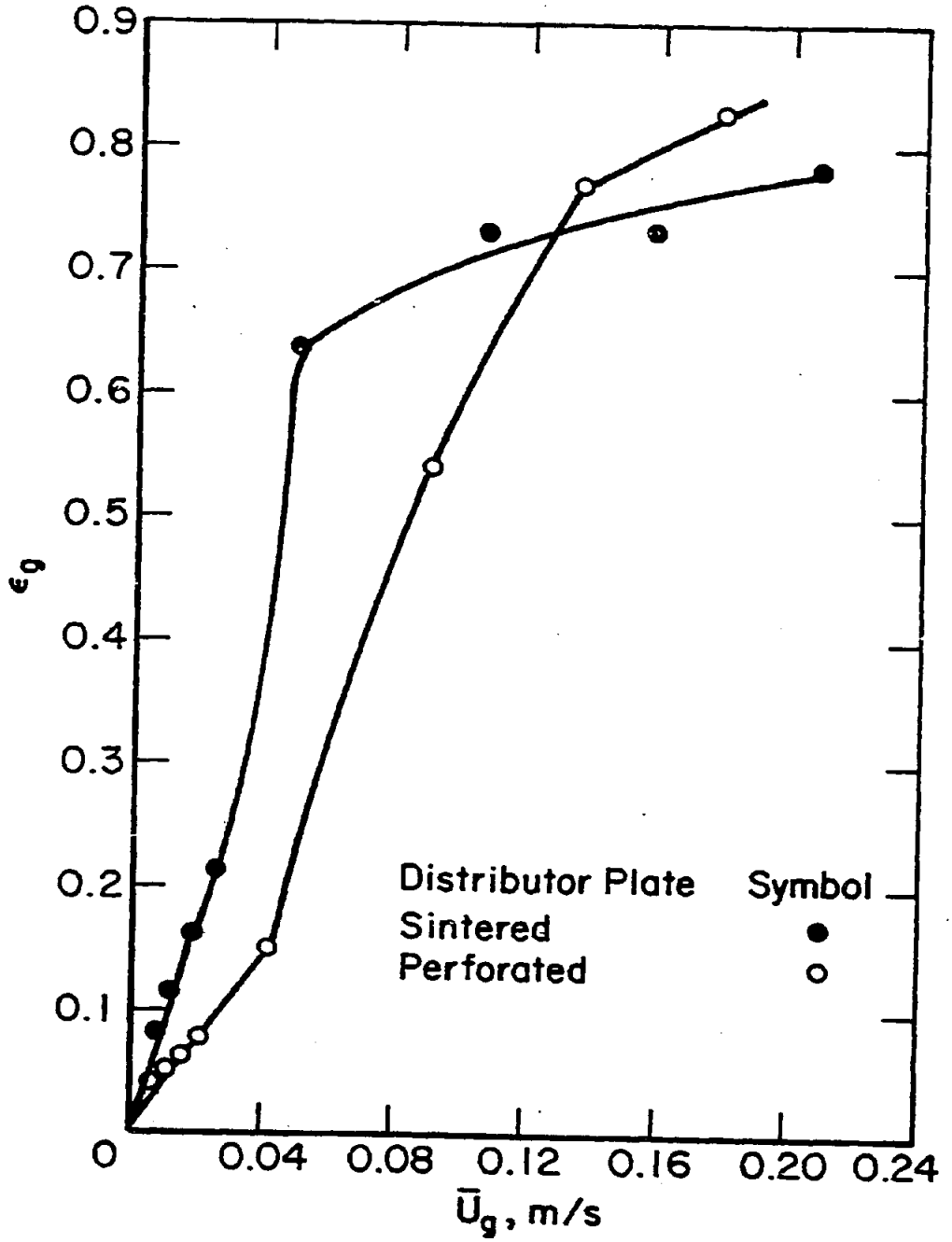

Figure 2. Effect of distributor type for foaming liquids (0.47 wt % ethanol/water).

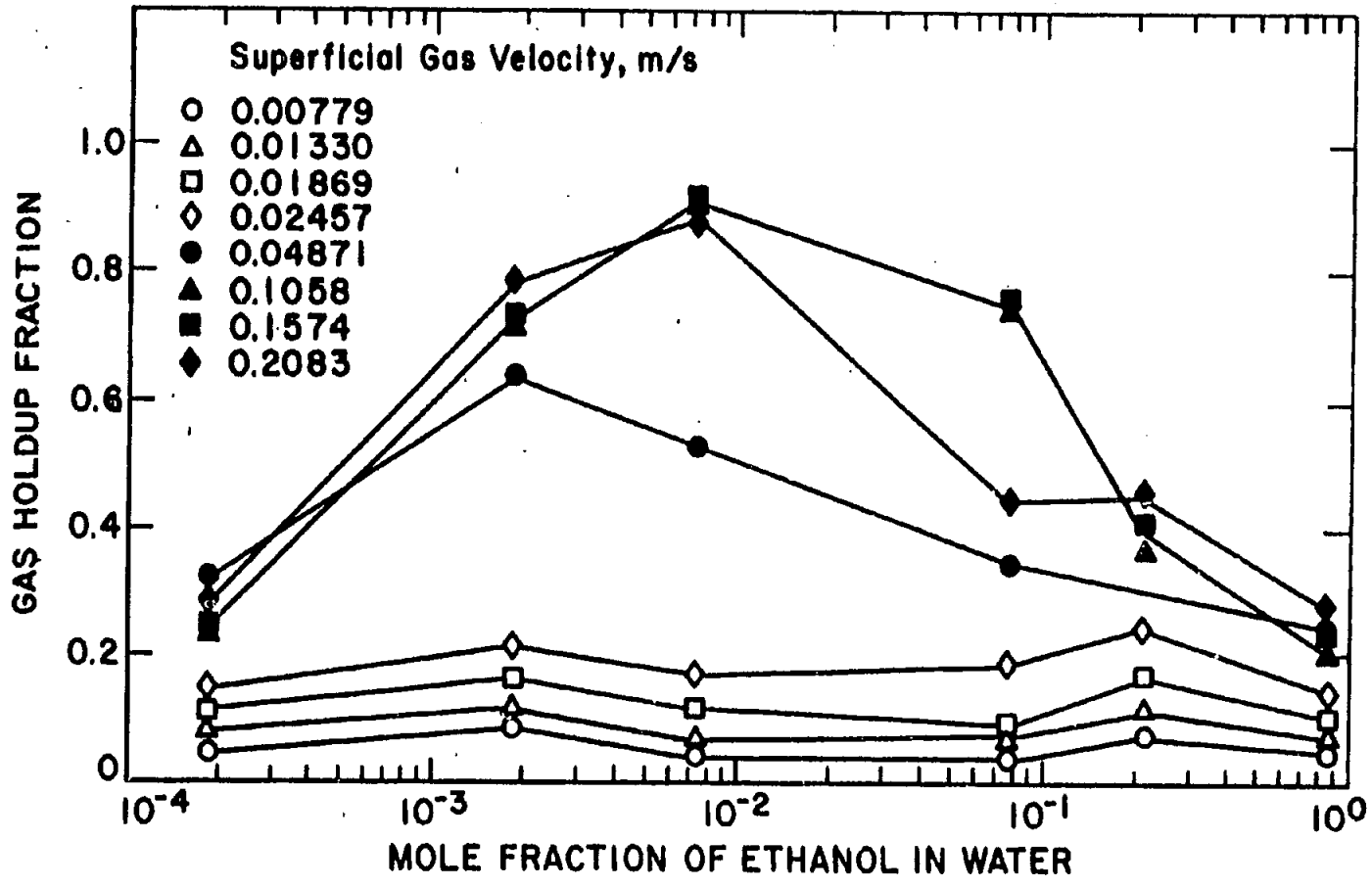

Figure 3. Effect of alcohol concentration on gas holdup [Shah et al., 1984]

BSI/5277

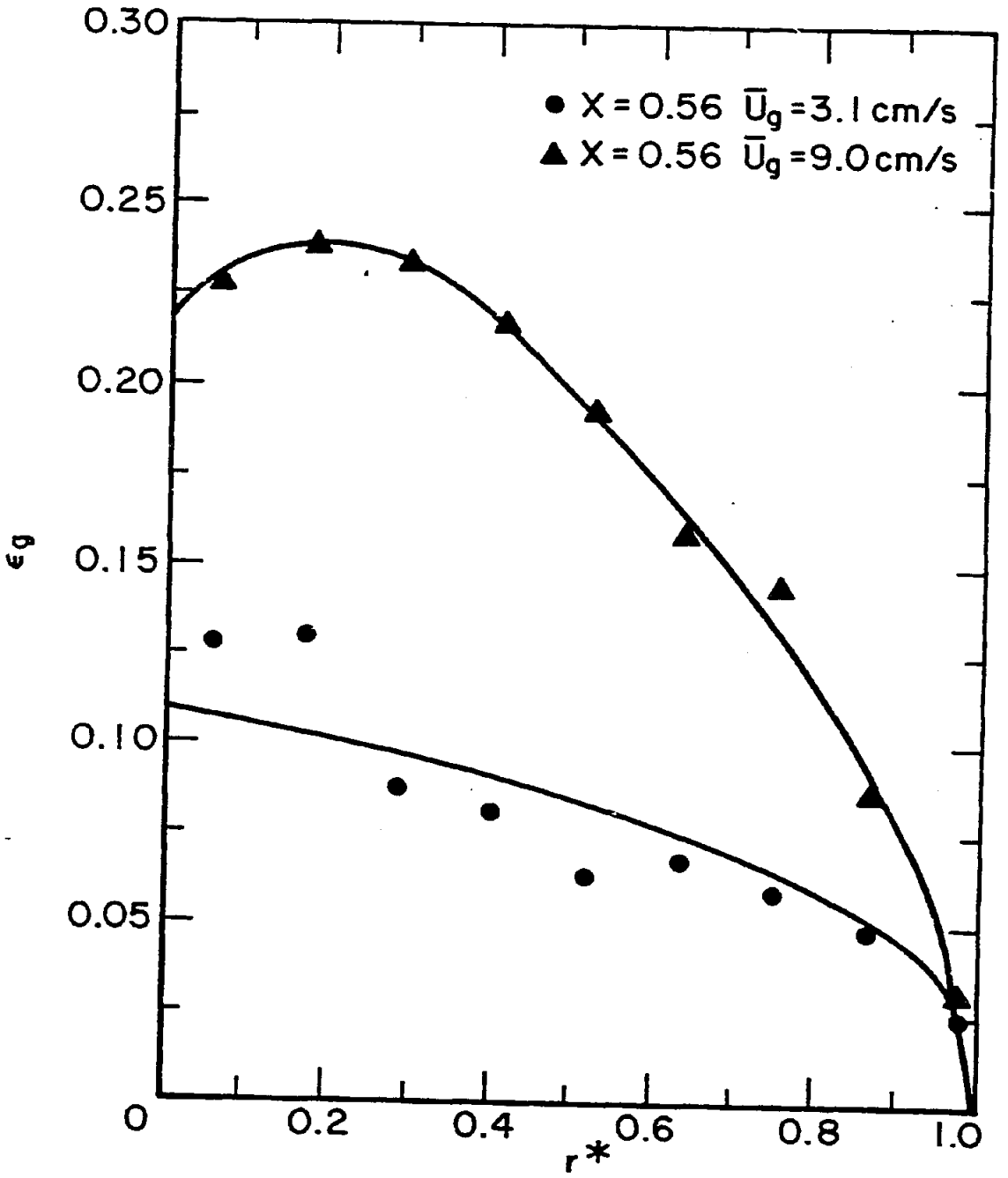

Figure 4. Radial gas holdup profile for N_2-H_2O system.

B&R/6576

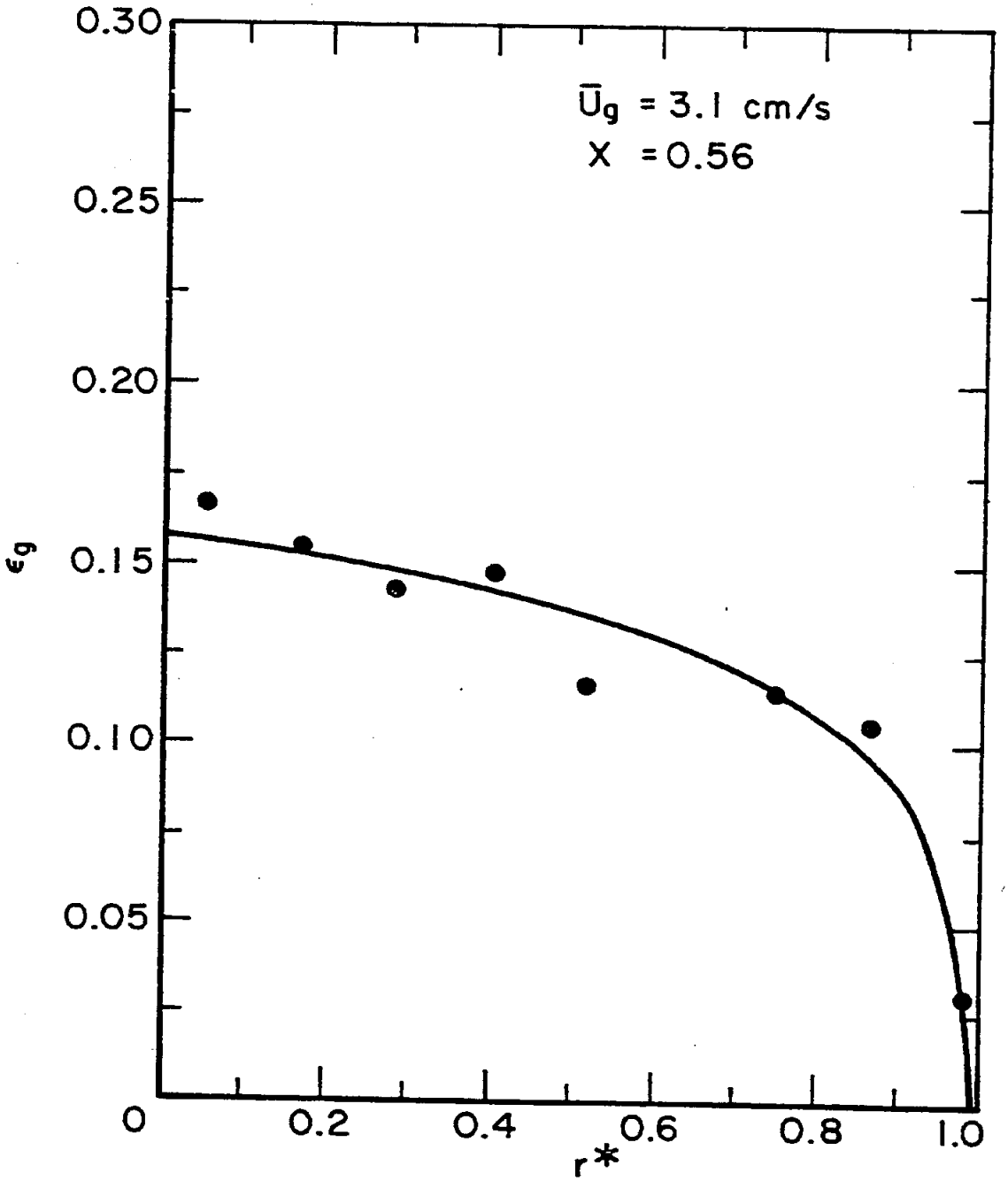

Figure 5. Radial gas holdup profile in 48 wt.% ethanol/water-nitrogen.

B&R/6578

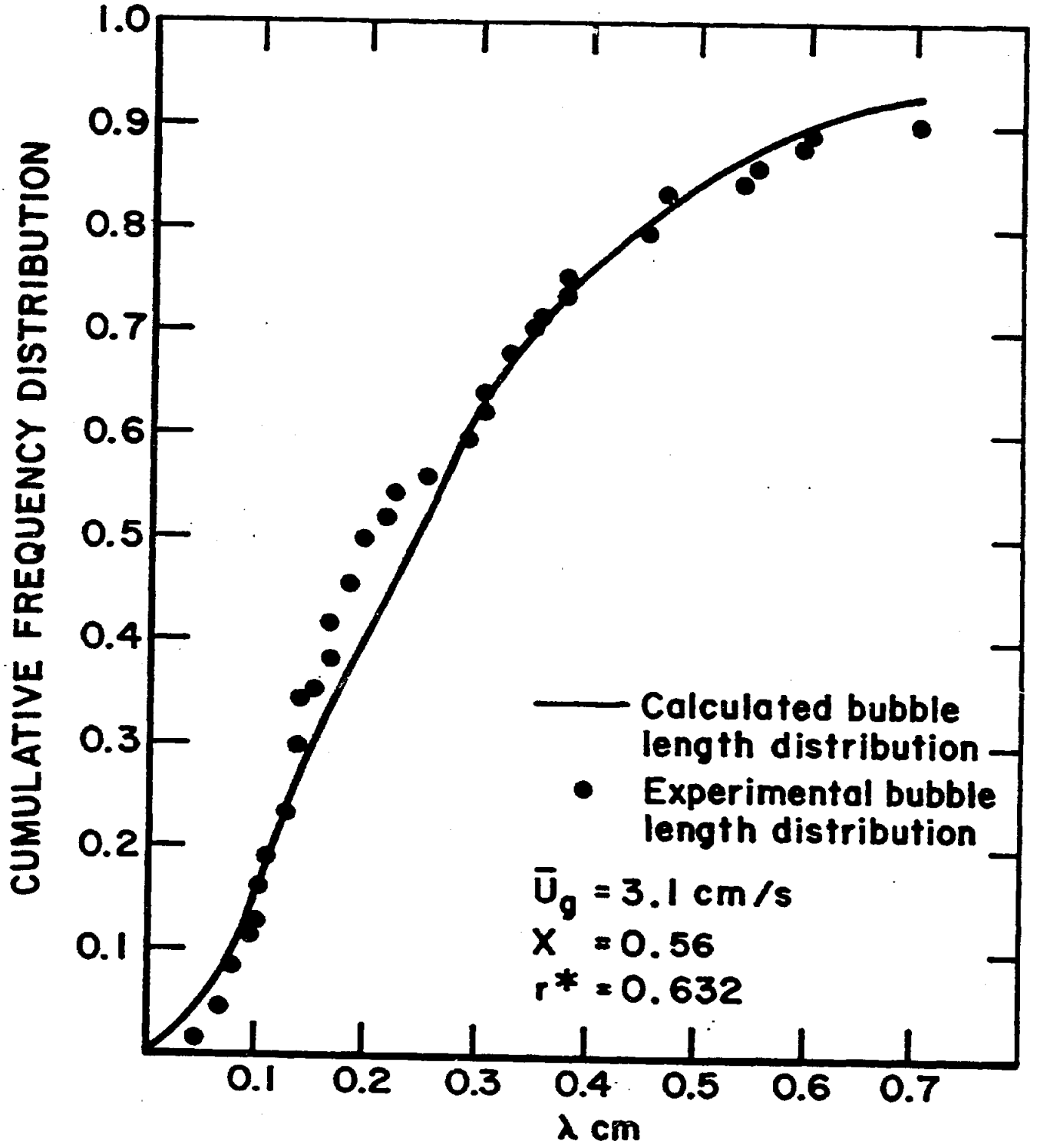

Figure 6. Cumulative frequency distribution of bubble length in N_2-H_2O system.

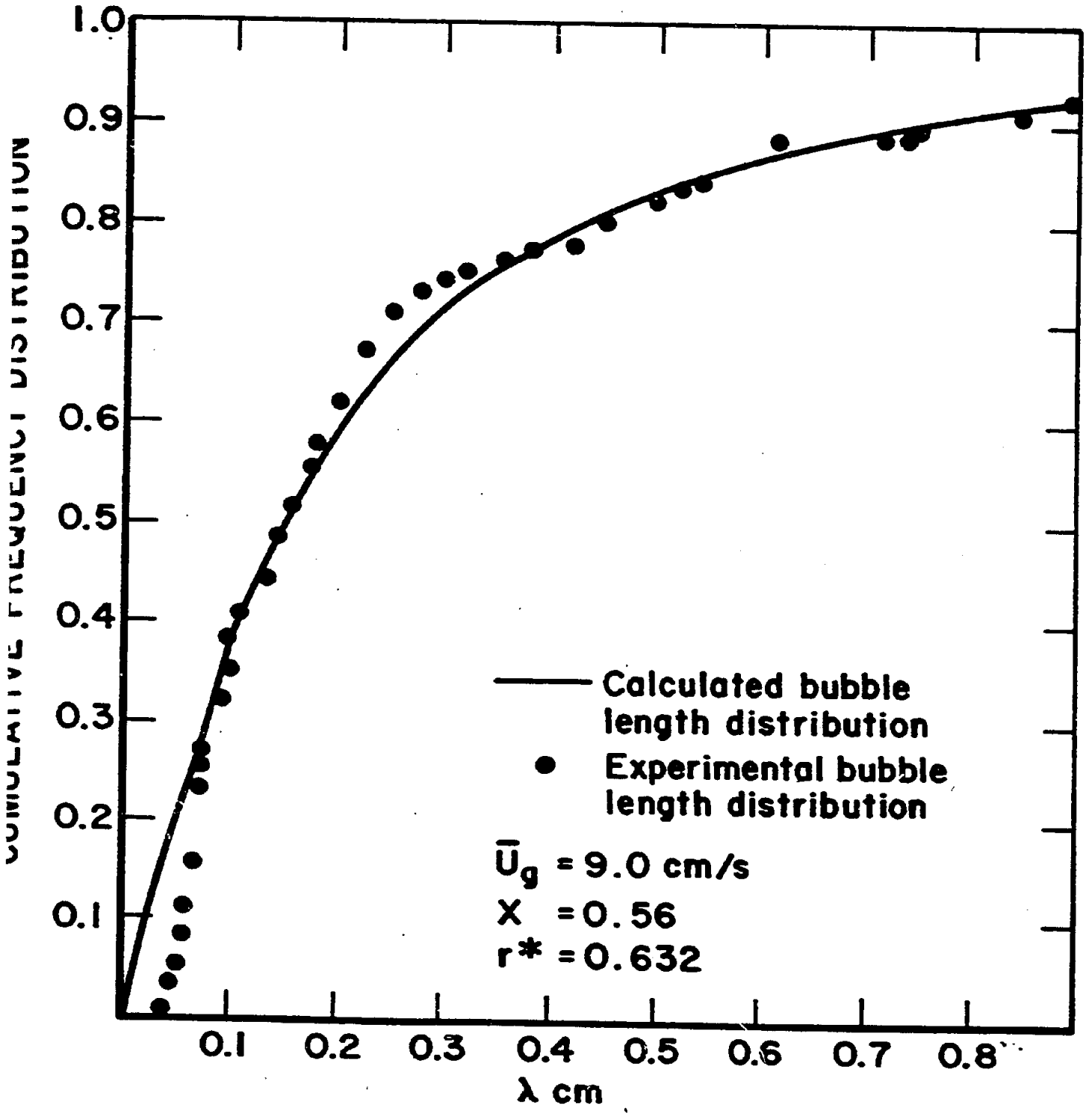

Figure 7. Cumulative frequency distribution of bubble length in N_2-H_2O system.

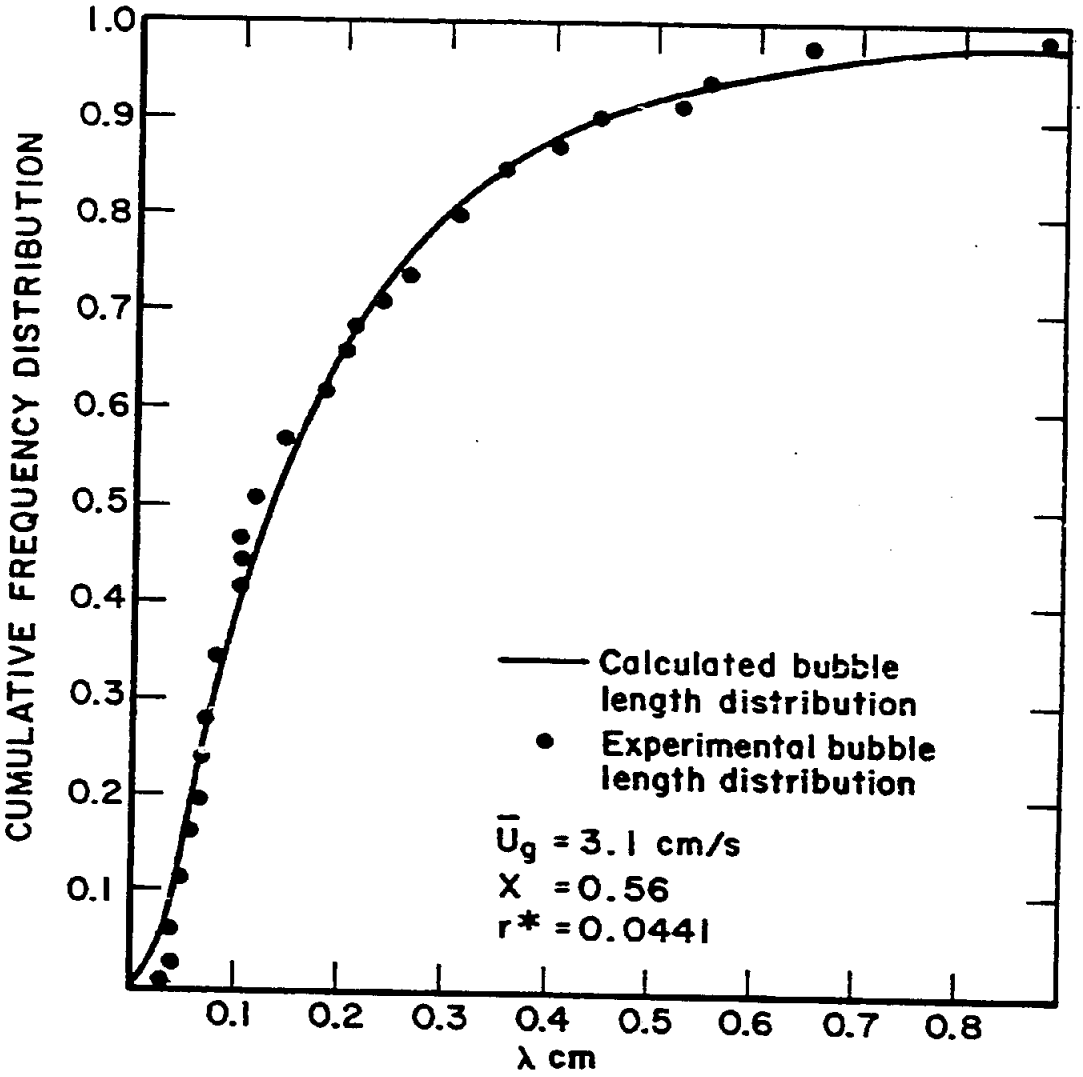

Figure 8. Cumulative frequency distribution of bubble length in 48 wt % ethanol/water-nitrogen system.

B&R/6587

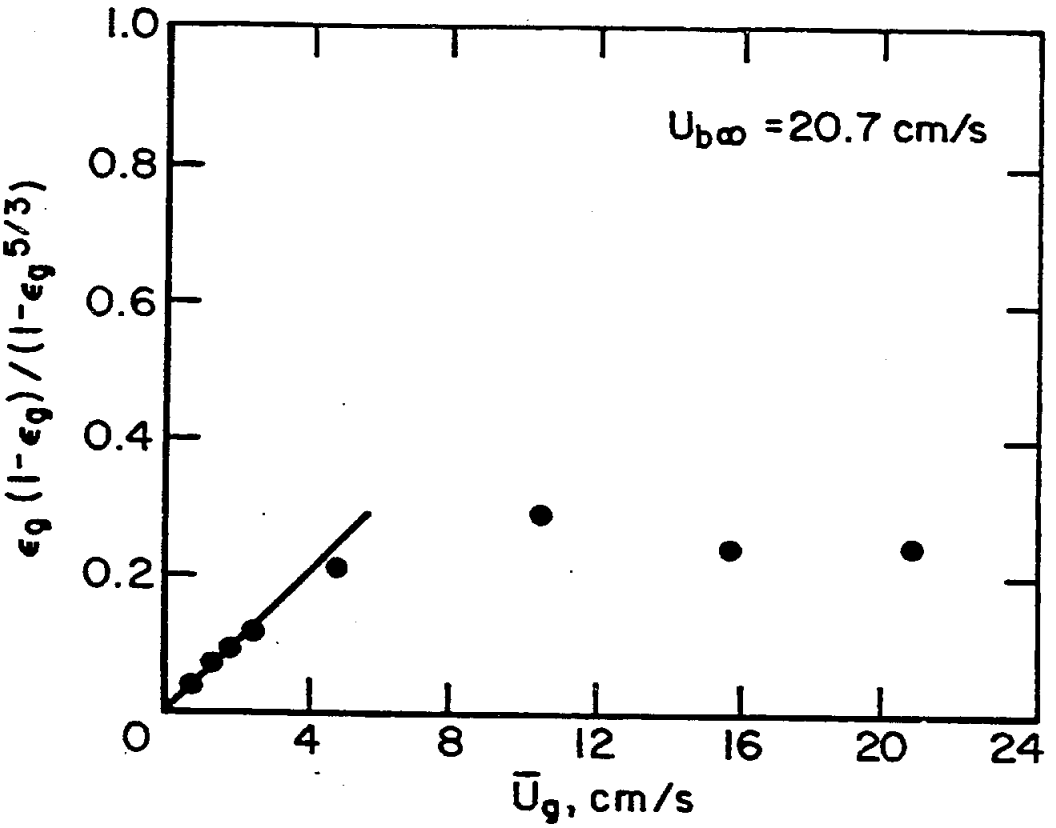

Figure 9. Determination of terminal bubble velocity for water system.

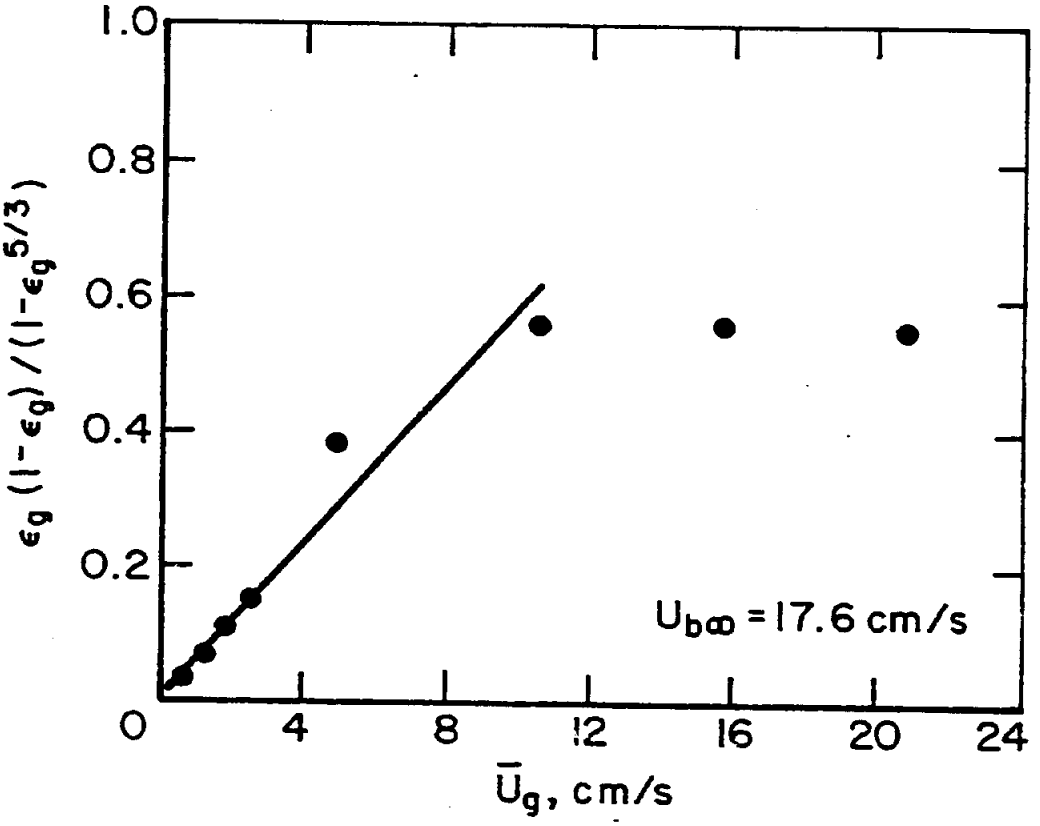

Figure 10. Determination of terminal bubble velocity for 1.8-wt % ethanol/ water system.

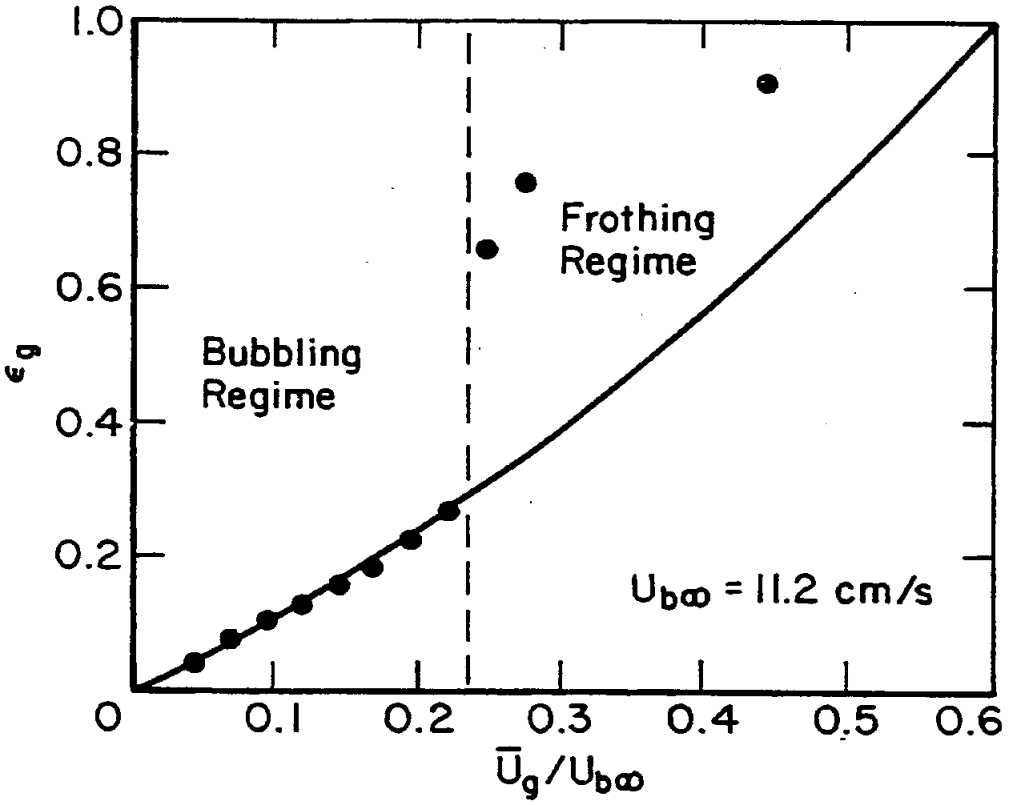

Figure 11. Correlation of gas holdup fraction in the bubble flow regime for 0.5-wt % butanol/water system.

B&R/6572

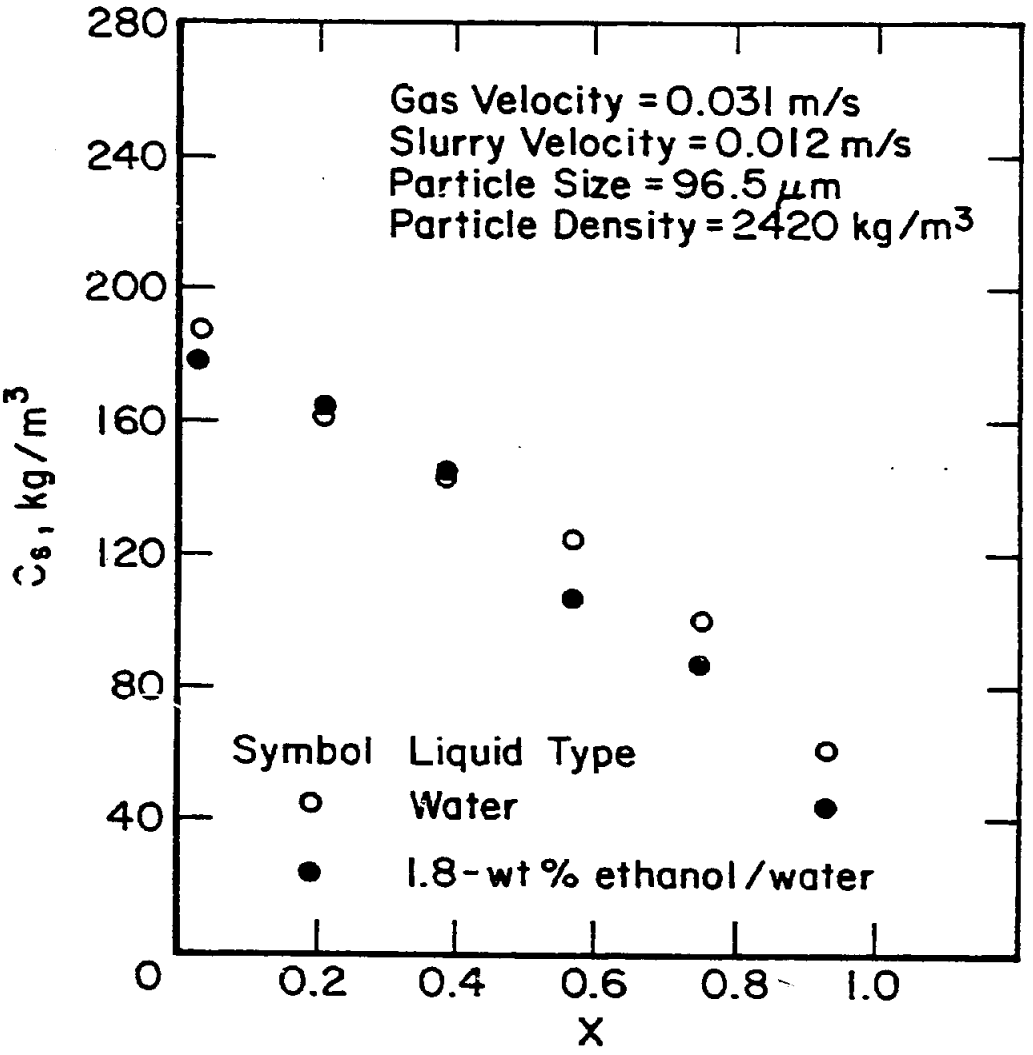

Figure 12. Effect of liquid properties on axial solids concentration distributions.

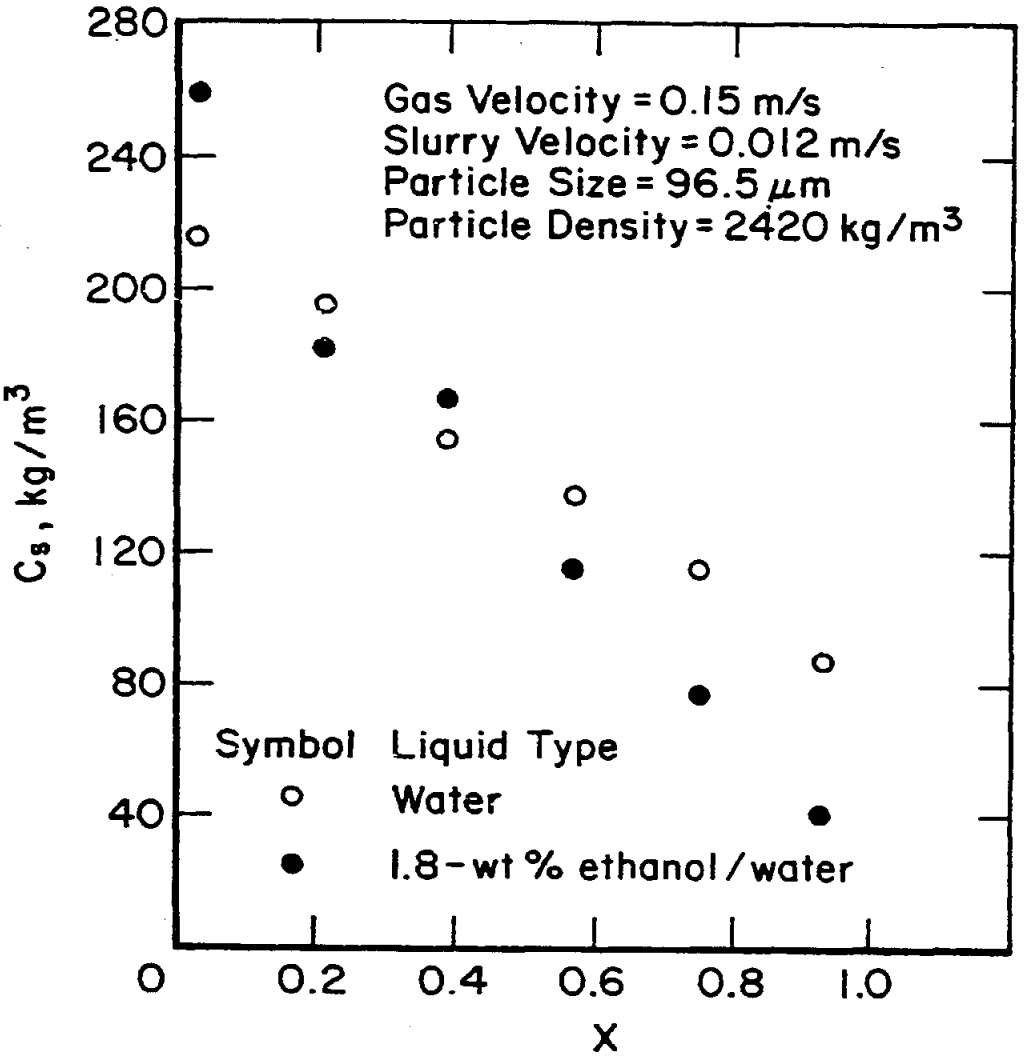

Figure 13. Effect of liquid properties on axial soiids concentration distributions.

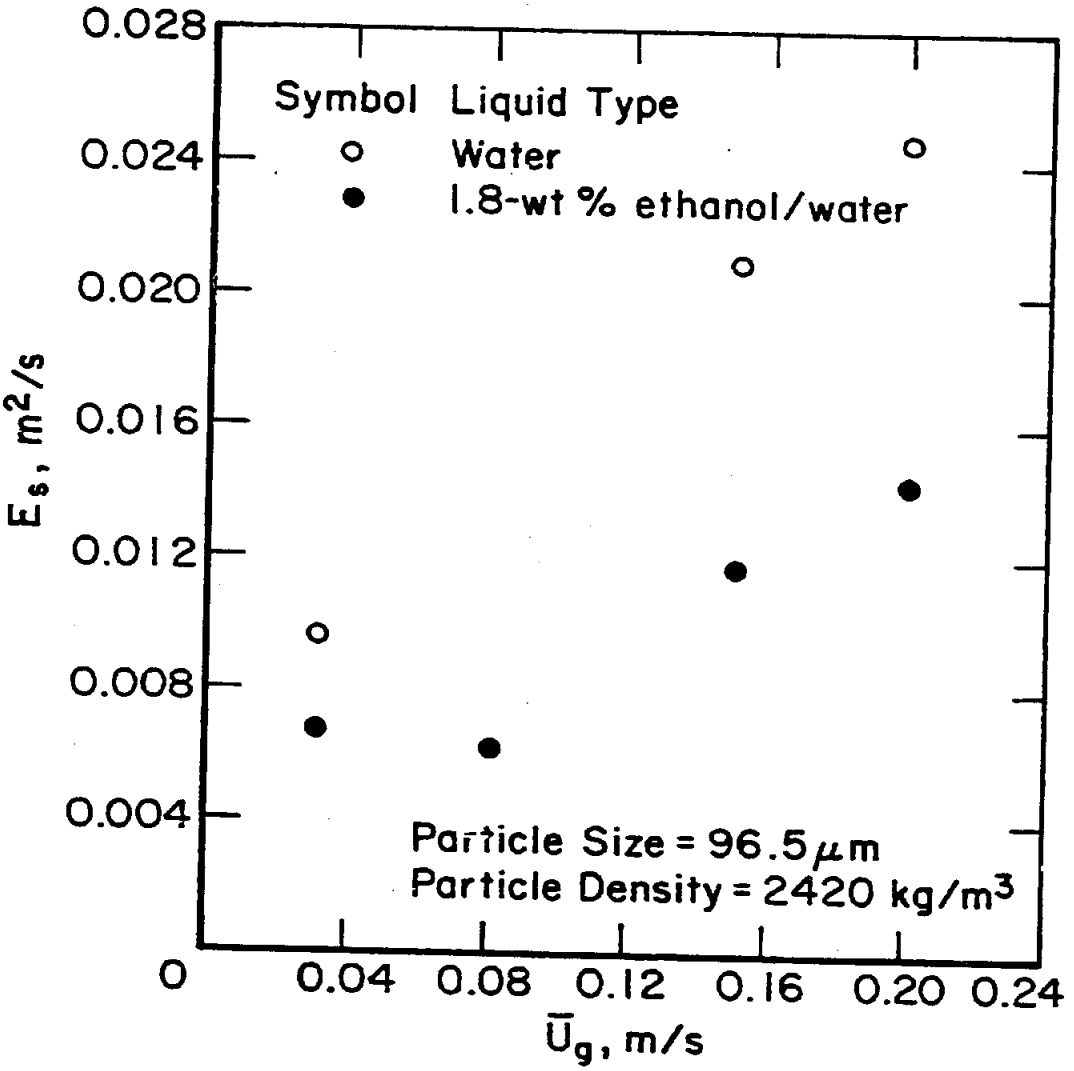

Figure 14. Effect of gas velocity and liquid type on solids dispersion coefficient.